Holographic Laser Oscillator Which Adaptively Corrects for Polarization and Phase Distortions

R. P. M Green,[1] D. Udaiyan,[1] G. J. Crofts,[1] D. H. Kim,[1,2] and M. J. Damzen[1,*]

[1]*Laser Physics Group, The Blackett Laboratory, Imperial College, London SW7 2BZ, United Kingdom*

[2]*Division of Electronics and Information Technology, Korea Institute of Science and Technology, P.O. Box 131, Cheongryang, Seoul, Korea*

(Received 25 July 1996)

A solid-state laser resonator is demonstrated which incorporates a real-time holographic element that corrects dynamically for both intracavity phase and polarization distortions. The results are compared with those from a holographic laser which corrects for phase distortions but does not include polarization correction. In comparison to the latter system the polarization correcting laser displays superior performance and notably, an output beam quality and energy that is insensitive to changes in intracavity polarization distortions. [S0031-9007(96)01463-9]

PACS numbers: 42.40.Eq, 42.65.Hw, 42.81.Gs

High average power solid-state laser oscillators are generally limited in beam quality and efficiency due to thermally induced phase distortions and depolarization in the gain medium [1]. The most common approach to reducing these losses is to have a low power master oscillator producing a high quality beam, and to use a power amplifier geometry which includes polarization and phase corrective techniques to reduce the depolarization losses [2] in the high gain amplifiers. Some of these systems use phase conjugate techniques to correct for the phase distortions present in the amplifiers and avoid precise alignment requirements [3–5].

Phase conjugate techniques have also been incorporated in laser oscillators to compensate for phase distortions in the resonator [6–8]. This Letter presents results from a laser resonator which, for the first time to our knowledge, incorporates intracavity vectorial phase conjugation (VPC). Vectorial phase conjugation is an effective way of eliminating both phase and polarization distortions in optical systems [9–11] and has been performed in several different types of nonlinear media [12–17]. More recently VPC has been demonstrated in inverted Nd^{3+}:YAG [18] using a four-wave mixing scheme presented by Zel'dovich *et al.* [10] (see shaded area in Fig. 1). In this work, we demonstrate the scheme incorporated into an adaptive holographic resonator [19] that uses the gain medium itself as the dynamic holographic element to provide correction for both polarization and phase distortions which are present in the oscillator. The operational requirements for the process of VPC in our system also have the effect of Q-switching the cavity resulting in short high peak power pulses, and spectrally narrowing the laser radiation to give single longitudinal mode (SLM) operation [19].

A schematic of the experimental system is shown in Fig. 1 with the key component, the VPC four-wave mixing arrangement, highlighted by the shading. This geometry uses counterpropagating pump beams $(\underline{E}_1, \underline{E}_2)$ that have orthogonal-circular polarization and a probe beam $[\underline{E}_3(\underline{r})]$ which can be of arbitrary, spatially varying polarization. A coherent interaction between the pump and probe beams produces population gratings (transmission and reflection [20]) in the gain medium. One of these gratings, the transmission grating formed by beams $\underline{E}_1$ and $\underline{E}_3$, is illustrated in Fig. 1. The combined Bragg-matched diffraction of radiation [20] from these gratings forms a beam $\underline{E}_4$ which is the vectorial phase conjugate of the probe $\underline{E}_3$, i.e., $\underline{E}_4(\underline{r}) \propto [\underline{E}_3(\underline{r})]^*$. The use of two quarter-wave plates to achieve counterpropagating orthogonally circularly polarized beams in laser resonators is a common technique to prevent spatial hole burning and the associated mode hopping of the lasing frequency [21,22]. In our system, however, it also provides the necessary conditions to achieve VPC [9] and thereby correct for polarization distortions within the loop.

The two laser amplifiers shown in Fig. 1 were flashlamp pumped Nd^{3+}:YAG rods which were time synchronized and operated at a repetition rate of 10 Hz. The holographic amplifier had a single-pass small-signal gain of $g_0 \sim 30$ and the power amplifier a larger gain of $g_0 \sim 70$. The nonreciprocal transmission element (NRTE) consisted of a Faraday rotator (FR) and half-wave plate (HW2) surrounded by a pair of Glan-air polarizers (P1, P2). The purpose of the NRTE is to provide near-unity transmission in the lasing (anticlockwise direction) and low transmission in the clockwise direction. The low clockwise transmission ensures that, when the system is lasing, beam $\underline{E}_3$ is similar in strength to the pump beams $(\underline{E}_1, \underline{E}_2)$ for optimum grating formation in the holographic amplifier. The high anticlockwise transmission ensures that the energy is extracted in the anticlockwise (conjugate) direction. The output coupler (OC) had a reflectivity of $R = 10\%$. By placing an aperture in the cavity, near to the output coupler, the laser was made to operate on a TEM_{00} spatial mode. This reduced the accessible gain volume and hence the energy available to the oscillating mode, but stabilized the fluctuations in the output energy on a shot-to-shot basis.

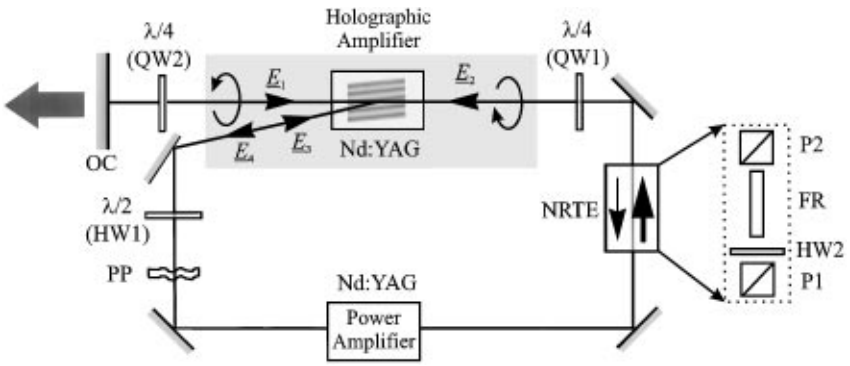

FIG. 1. Schematic of the VPC holographic laser oscillator. OC: output coupler; QW1, QW2: quarter-wave plates; HW1, HW2: half-wave plates; FR: Faraday rotator; P1, P2: polarizers; NRTE: nonreciprocal transmission element; PP: phase plate.

The holographic laser operates in the same manner as a previously reported system [19] which did not include the quarter-wave plates (QW1, QW2). Lasing action starts from noise with weak gain gratings being induced by the spontaneous emission. These gratings weakly diffract radiation in the loop, causing enhancement of the amplified spontaneous emission flux. Diffracted intracavity radiation that gives constructive interference to enhance the growth of the grating will be preferentially selected. This parametric feedback, involving the mutual growth of the grating and the fields, leads to the formation of a laser oscillator with spatial and spectral selectivity.

Initially, to quantify the effects of intracavity polarization distortion without correction, the quarter-wave plates (QW1, QW2) were removed from the cavity. A half-wave plate (HW1) was inserted into the feedback arm to act as a polarization distorting element. The p-polarized radiation extracted at the output coupler and the returning s-polarized (uncorrected) component ejected at polarizer P1 were monitored for various angles of the half-wave plate and the results are presented in Fig. 2. It can be seen from Fig. 2 that the output of the nonpolarization correcting system varies periodically as the half-wave plate is rotated. At an angle of zero degrees, the probe beam ($\underline{E}_3$) passes through an axis of the wave plate and so is not rotated. Therefore, the probe and pump beams are all p polarized resulting in the efficient formation of both transmission and reflection holograms [20] and hence, optimal lasing can occur producing an output pulse of 40 mJ. This is lower than in a previously reported experiment [19] due to the lower small-signal gain of the two amplifiers. As the polarization state of the probe is rotated by the half-wave plate, the component of p polarization in the probe beam is reduced. This results in a lower diffraction efficiency of the holographic gain gratings and a reduction in the output energy. Lasing is inhibited when the half-wave plate is rotated to 45° (beam $\underline{E}_3$ becomes s polarized and orthogonal to the pump beams) and no gain grating can be formed.

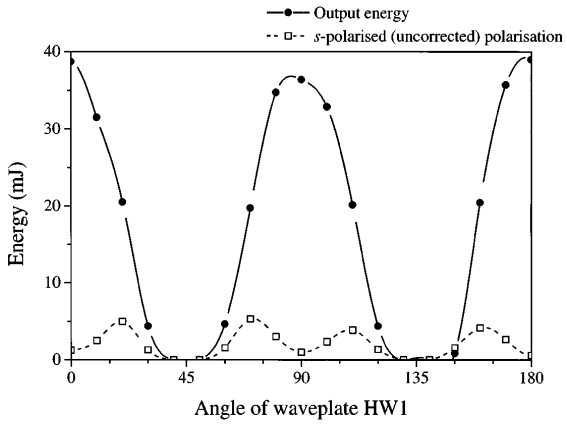

FIG. 2. The output (p-polarized) energy and ejected (s-component) energy as a function of the angle of the half-wave plate (HW1) for the nonpolarization correcting holographic resonator (without the presence of the quarter-wave plates).

Figure 2 also shows the energy of the uncorrected (s-polarized) component of $\underline{E}_4$ as a function of the wave plate angle. The periodic variation in energy with the wave plate angle displays twice the frequency as compared to the p-polarized component. This behavior can be explained by noting that, regardless of the polarization state of the probe $\underline{E}_3$, the diffracted conjugate $\underline{E}_4$ is always p polarized before passing through the half-wave plate (HW1) as a result of being generated by diffraction of the p-polarized pump beams $\underline{E}_1$, $\underline{E}_2$. The ejected (uncorrected) s-polarized component of beam $\underline{E}_4$ minimizes when the half-wave plate is at 0° or 90° ($\underline{E}_3$ is p polarized) and also falls to zero when the half-wave plate approaches 45°, since lasing is then inhibited. The ejected s component maximizes at intermediate wave plate angles where there is a tradeoff between the overall level of intracavity flux, which reduces as the diffraction efficiency falls, and the increasingly large component of $\underline{E}_4$ that is uncorrected (rotated to the s-polarization state).

The polarization-correcting system was then assembled by incorporating the quarter-wave plates, as shown in Fig. 1. The presence of two, coaligned polarizing cubes in the NRTE defines the polarization state (linear) of radiation in this part of the cavity. To achieve the circularly polarized pump beam $\underline{E}_2$, a quarter-wave plate

(QW1) was placed between the holographic amplifier and polarizer P2 and orientated such that the linearly p-polarized radiation from polarizer P2 is 45° to the wave plate axes. The counterpropagating orthogonally polarized beam $\underline{E}_1$ was achieved by placing another quarter-wave plate (QW2) near the output coupler. The double pass of the quarter-wave plate (QW2) results in an orthogonally circularly polarized pump beam at the Nd^{3+}:YAG amplifier, regardless of its orientation angle. The orientation of the wave plate could, however, be used to control the angle of the linearly polarized output beam from the resonator. The pump beams ($\underline{E}_1$ and $\underline{E}_2$) are forced to be orthogonally circularly polarized, by the presence of the two quarter-wave plates (QP1 and QP2), as this is a necessary condition for vectorial phase conjugation to be achieved in an isotropic medium [9]. The output energy and depolarized (s-polarized) component of the VPC laser were then monitored for various angles of the half-wave plate, in an identical manner to the non-VPC scheme, and the results are presented in Fig. 3.

It can be seen that, unlike the non-VPC laser, the output of the VPC laser did not fall to zero as the wave plate was rotated, demonstrating that the laser system adapts to the depolarizing element (HW1). The output energy varied from an average of 28 mJ per pulse by a standard deviation of ±4%. It is noted that this output is lower than the peak output of 40 mJ from the noncorrecting system. This is due to more efficient grating formation when all the beams are of the same polarization state.

Figure 3 also shows that there is only a small level of ejected s-polarized component and which was relatively insensitive to the wave plate orientation indicating good polarization distortion correction. The small level of ejected s-polarized radiation can be accounted for by a thermally induced depolarization of the pump beams in the holographic amplifier, which does not alter as the depolarizer (HW1) is rotated and cannot, therefore, be corrected for by this system. This depolarization is also present in the standard holographic resonator which does not contain quarter-wave plates. The effect of thermal birefringence in the adaptive element could be minimized by using a low gain holographic amplifier which would further improve the fidelity of the VPC. The lasing efficiency could then be maintained by using a higher gain power amplifier and any increase in the depolarization due to this element would be corrected for.

As with the standard holographic resonator, the VPC holographic resonator also has the ability to correct for phase aberrations present in the loop. Figure 4(a) shows a typical spatial profile of the output from the laser system using a charge-coupled device (CCD) camera. To test the phase corrective properties of the laser, a glass plate (PP) that had been etched in HF acid was inserted into the cavity to provide severe phase distortions. In order to prevent the loss of spatial information from the highly divergent radiation, the plate was placed close to the holographic amplifier rod to provide good spatial overlap with the pump beams. If an appropriate imaging lens was incorporated in the system, to collect the diffracted radiation, the plate could then be placed anywhere within the loop. Figure 4(b) shows the spatial output of the VPC laser with the phase plate (PP) present in the loop. It can be seen that the spatial profile of the output remained unchanged indicating that the phase distortions introduced by the etched glass plate were compensated for. To indicate the severity of the phase distortions due to the glass plate, a TEM_{00} beam was passed through it and the distorted spatial profile of the beam recorded on a CCD camera. An example of the distorted beam shape is shown in Fig. 4(c) and can be seen to be highly aberrated compared to Figs. 4(a) and 4(b).

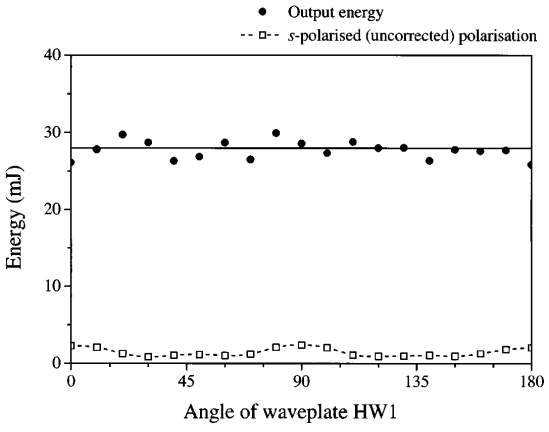

FIG. 3. The output energy and s-component energy as a function of the angle of the half-wave plate (HW1) polarization distorter for the VPC holographic resonator.

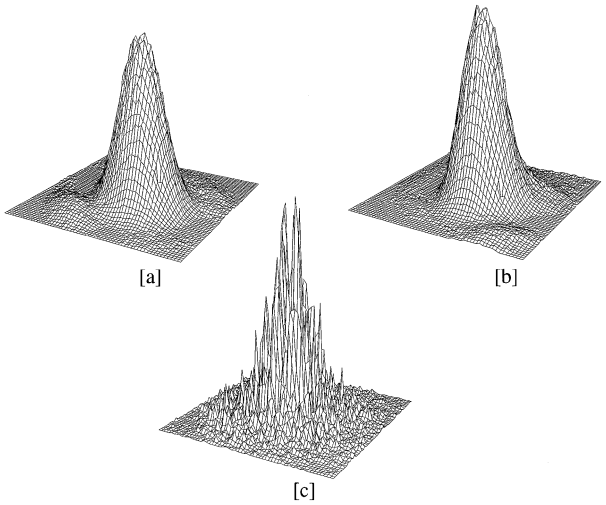

FIG. 4. Spatial output of the VPC laser, (a) without distortions, (b) when the phase distortions are placed in the loop, and (c) is the spatial profile of a Gaussian beam after single passage through the phase distortions.

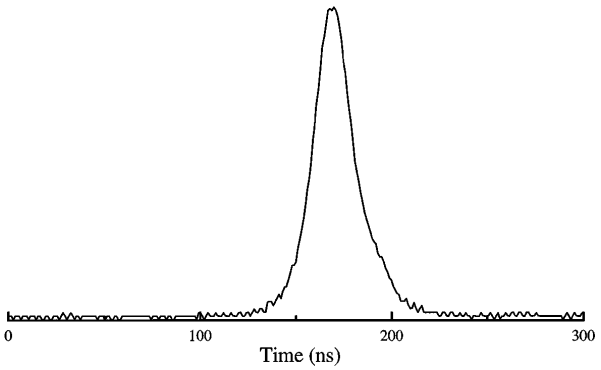

FIG. 5. A temporal profile of the output of the VPC holographic laser resonator showing a smooth pulse of duration 23 ns (FWHM) and single longitudinal mode.

A temporal profile of the laser output is presented in Fig. 5 and shows the radiation to be in the form of a pulse of duration 23 ns FWHM and which was spectrally analyzed to be single longitudinal mode (SLM). The short duration is caused by an effective passive Q-switching of the system due to the self-enhancement and erasure of the population gratings by the lasing radiation and also the subsequent depletion of the stored gain in the power amplifier, when lasing commences. The coherence requirements for the formation of the gain gratings and the spectral selectivity of the gain hologram constrain the laser to operate narrow band resulting in a near-transform-limited SLM pulse. Occasionally a pulse with a small temporal modulation of 6 ns is seen, indicating a weak second mode at a mode spacing of 167 MHz and corresponding to the loop length of 180 cm formed by the transmission grating.

In conclusion, we have demonstrated a laser system which corrects for both polarization and phase distortions that are present in the cavity. These types of aberrations can severely reduce the performance of conventional lasers. In addition, due to the dynamic buildup and selectivity of the gain holograms that are formed, the laser produces a Q-switching SLM pulse without the presence of conventional switching or frequency selective elements.

*Electronic address: m.damzen@ic.ac.uk FAX: (+44) 171 594 7744.

[1] W. Koechner, *Solid-State Laser Engineering* (Springer-Verlag, Berlin, Heidelberg, 1992), p. 393.
[2] W. C. Scott and M. de Wit, Appl. Phys. Lett. **18**, 3 (1971).
[3] I. D. Carr and D. C. Hanna, Appl. Phys. B **36**, 83 (1985).
[4] N. F. Andreev, E. A. Khazanov, S. V. Kuznetsov, G. A. Pasmanik, E. I. Shklovsky, and V. S. Sidorin, IEEE J. Quantum Electron. **27**, 135 (1991).
[5] N. F. Andreev, S. V. Kuznetsov, O. V. Palshov, G. A. Pasmanik, and E. A. Khazanov, Sov. J. Quantum Electron. **22**, 800 (1992).
[6] V. I. Bezrodnyi, F. I. Ibraginov, B. I. Kislanko, R. A. Petrenko, V. L. Strizhevskii, and E. A. Tichonov, Sov. J. Quantum Electron. **10**, 382 (1980).
[7] N. N. Il'ichev, A. A. Malyutin, and P. O. Pashinin, Sov. J. Quantum Electron. **12**, 1161 (1982).
[8] I. M. Bel'dyugin, B. Ya Zel'dovich, M. V. Zolotarev, and V. V. Shkunov, Sov. J. Quantum Electron. **15**, 1583 (1985).
[9] R. W. Boyd, *Nonlinear Optics* (Academic Press, Boston, 1992), p. 254.
[10] B. Ya Zel'dovich and V. V. Shkunov, Sov. J. Quantum Electron. **9**, 379 (1979).
[11] B. Ya Zel'dovich and T. V. Yakovleva, Sov. J. Quantum Electron. **10**, 501 (1980).
[12] N. G. Basov, V. F. Efimkov, I. G. Zubarev, A. V. Kotov, S. I. Mikhailov, and M. G. Smirnov, JETP Lett. **28**, 197 (1978).
[13] G. Martin, L. K. Lam, and R. W. Hellwarth, Opt. Lett. **5**, 185 (1980).
[14] M. Ducloy and D. Bloch, Phys. Rev. A **30**, 3107 (1984).
[15] I. McMichael, P. Yeh, and P. Beckwith , Opt. Lett. **12**, 507 (1987).
[16] M. S. Malcuit, D. J. Gauthier, and R. W. Boyd, Opt. Lett. **13**, 663 (1988).
[17] E. J. Miller, M. S. Malcuit, and R. W. Boyd, Opt. Lett. **15**, 1188 (1990).
[18] R. P. M. Green, S. Camacho-Lopez, and M. J. Damzen, Opt. Lett. **21**, 1214 (1996).
[19] M. J. Damzen, R. P. M. Green, and K. S. Syed, Opt. Lett. **20**, 1704 (1995).
[20] R. P. M. Green, G. J. Crofts, and M. J. Damzen, Opt. Commun. **102**, 288 (1993).
[21] H. Haken and H. Sauermann, Z. Phys. **173**, 261 (1963).
[22] C. L. Tang, H. Statz, and G. De Mars, J. Appl. Phys. **34**, 2289 (1963).